A photon assembly line on a semiconductor quantum well

C. Rocke, A. O. Govorov, Achim Wixforth, Jörg P. Kotthaus, G. Böhm, G. Weimann

Angaben zur Veröffentlichung / Publication details:

Rocke, C., A. O. Govorov, Achim Wixforth, Jörg P. Kotthaus, G. Böhm, and G. Weimann. 1997. "A photon assembly line on a semiconductor quantum well." *physica status solidi a* 164 (1): 535–40. https://doi.org/10.1002/1521-396X(199711)164:1%3C535::AID-PSSA535%3E3.0.CO;2-P.

A Photon Assembly Line on a Semiconductor Quantum Well

C. Rocke (a), A. O. Govorov (a), A. Wixforth (a), J. P. Kotthaus (a), G. Böhm (b), and G. Weimann[1]) (b)

(a) Sektion Physik der LMU, Geschwister-Scholl-Platz 1, D-80539 München, Germany

(b) Walter-Schottky-Institut, Technische Universität München, Am Coulombwall, D-85748 Garching, Germany

The lateral potential superlattice accompanying a surface acoustic wave on a semiconductor quantum well structure is employed to efficiently transform light into a long-lived electron–hole polarization that can be reassembled into photons after very long storage times. Both the location of the emission process on the sample and the storage-time can be chosen at will as the dynamical superlattice is able to transport the photogenerated excitations over macroscopic distances across the semiconductor sample. The ionization process of the photogenerated excitons in the piezoelectric fields of the sound wave can be directly observed by the absorption of a second sound wave probing the areal conductivity of the photogenerated charges.

The optoelectronic properties of semiconductor structures with reduced dimensionality have attracted tremendous interest over the last decade or so [1,2]. State of the art band-gap engineering technologies enable us to tailor semiconductor systems with desirable optoelectronic properties and study fundamental aspects of carrier dynamics. This has increased our fundamental understanding of the dynamic properties of artificial semiconductor structures and also resulted in a wide range of novel devices such as quantum well lasers, modulators and detectors as well as all-optical switches [3]. Strong electric fields lead to further modifications of the optical properties of these engineered semiconductors and provide an additional flexibility in their design. However, the strength of the interband transitions in these devices seems to be dominated by the atomic-like Bloch parts of the wavefunctions and thus by the bulk band structure of the semiconductor [4]. Thus it appears unavoidable that strong interband optical transitions are linked to direct band gap semiconductors with short radiative lifetimes such as GaAs whereas long radiative lifetimes of photogenerated carriers imply utilization of semiconductors with indirect band gaps such as Si and correspondingly reduced interband absorption. Earlier attempts to combine strong interband absorption with long radiative lifetimes have focused on so-called doping superlattices [5] where alternating n- and p-doping along the growth direction is used to combine a direct gap in momentum space with an indirect gap in real space. The resulting spatial separation of photogenerated electron–hole (e–h) pairs yields considerably prolonged lifetimes. More recently it was shown that static electric fields associated with tunable *lateral* potential superlattices

[1]) Present address: Fraunhofer Institut IAF, D-79108 Freiburg, Germany.

parallel to a quantum well may result in pronounced modifications of the interband optical properties and may lead to prolonged radiative lifetimes [6,7].

Here, we employ a moving lateral potential superlattice to separate and efficiently store and transport photogenerated e–h pairs along the plane of a semiconductor quantum well [8]. We show that the confinement of photogenerated e–h pairs to two dimensions together with the moving lateral superlattice allows reversible charge separation.[2]) We demonstrate that a strong interband absorption in combination with extremely long lifetimes of the optical excitations is possible without affecting the superior optical quality of the quantum well material.

The spatial separation of the electron–hole pairs is achieved via the piezoelectric potential of acoustic waves propagating along the surface of a semiconductor quantum well system. On a piezoelectric substrate, the elliptically polarized surface acoustic waves (SAWs) are accompanied by both lateral and vertical piezoelectric fields which propagate at the speed of sound. Those fields can be strong enough to field-ionize optically generated excitons and to confine the resulting electrons and holes in the moving lateral potential wells separated by one half wavelength of the SAW. The spatial separation dramatically reduces the recombination probability and increases the radiative lifetime by several orders of magnitude as compared to the unperturbed case. We further demonstrate that the dynamically trapped electron–hole pairs can be transported over macroscopic distances at the speed of sound and that deliberate screening of the lateral piezoelectric fields of the SAW leads to an induced radiative recombination after long storage times at a location remote from the one of e–h generation. This conversion of photons into a long lived e–h polarization which is efficiently reconverted into photons can serve as an optical delay line operating at sound velocities. The ionization process of the photogenerated excitons in the piezoelectric fields of the SAW can be directly observed by the absorption of a second sound wave probing the areal conductivity of the photogenerated charges.

The undoped quantum well samples used in our experiments are grown by molecular beam epitaxy on a (100) GaAs substrate. The quantum well consists of 10 nm pseudomorphic $In_{0.15}Ga_{0.85}As$ grown on a 1 μm thick GaAs buffer and is covered by a 20 nm thick GaAs cap layer. The active area of the sample is etched into a 2.5 mm long and 0.3 mm wide mesa (see inset of Fig. 1) with two interdigital transducers (IDTs) at its ends. The IDTs are designed to operate at a center frequency $f_{\mathrm{SAW}} = 841$ MHz. They are partially impedance matched to the 50 Ω radio frequency (RF) circuitry using an on- chip matching network thus reducing the insertion loss of each transducer to the 5 dB range. The sample is mounted in an optical cryostat and the experiments presented here are performed at $T = 4.2$ K. Light from a pulsed laser diode ($\lambda_{\mathrm{laser}} = 780$ nm) or from a tunable titanium–sapphire laser is used for optical interband excitation. The photoluminescence (PL) of the sample is analyzed in a triple grating spectrometer. Either a gated photomultiplier or a charged coupled device (CCD) serve as a detector for the PL. Application of a high frequency signal to one of the IDT launches a SAW of wavelength $\lambda_{\mathrm{SAW}} = v_{\mathrm{SAW}}/f_{\mathrm{SAW}}$. It propagates along the [110] direction and can be detected at the other IDT after the acoustic delay of order of 1 μs determined by the spacing of the IDTs. Here, $v_{\mathrm{SAW}} = 2865$ m/s denotes the SAW velocity for the given sample cut and orientation. Either pulsed or continuos wave (cw) operation of the SAW transducers is possible.

---

[2]) Transport oif unipolar charges in epitaxial films is usually referred to as acoustic charge transport (ACT), see, e.g. [10].

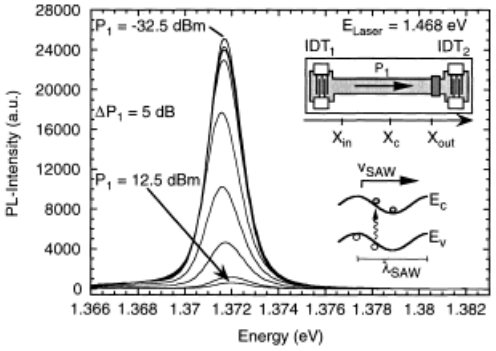

Fig. 1

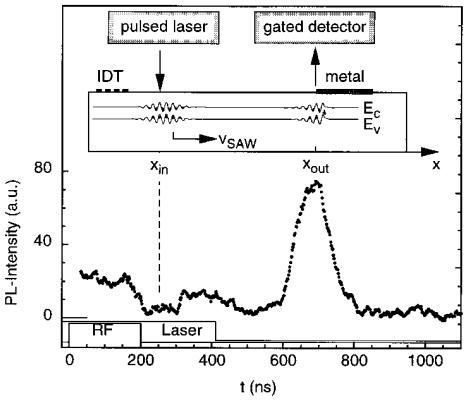

Fig. 2

Fig. 1. Photoluminescence spectra of a single 10 nm wide InGaAs/GaAs quantum well structure for different acoustic powers. The optical excitation occurs at the site $x = x_c$ with an intensity of 50 mW/cm^2 and energy $E_{\mathrm{Las}} = 1.468$ eV. The insets schematically depict the sample design with two interdigital transducers and the storage of optically generated excitons in the potential of a surface acoustic wave

Fig. 2. Ambipolar transport of trapped charges by a SAW. At $t = 0$ ns a 200 ns long RF pulse at $f_{\mathrm{SAW}} = 841.5$ MHz applied to IDT$_1$ generates a SAW packet with an acoustic power of $P_1 = 13.5$ dBm. At $t = t_1$ and $x = x_{\mathrm{in}}$ the potential extrema of the SAW are filled with photogenerated electron–hole pairs which are transported with sound velocity to a semitransparent metallization at $x = x_{\mathrm{out}}$. Here the deliberate screening of the piezoelectric potential modulation lifts the spatial separation of the carriers and induces radiative recombination at $x = x_{\mathrm{out}}$ and $t = t_2$. The duration of the RF pulse and the laser pulse are indicated in the lower part

In Fig. 1 we depict the 'direct', i.e. local and instantaneous PL of the quantum well under the influence of a SAW. Laser excitation and PL emission occur at the same site x_c on the sample close to the center of the mesa with the recombination time being much shorter than the time resolution of our experiment (20 ns). The different PL traces are recorded at different acoustic power levels P_1 of a cw high frequency ($f_{\mathrm{SAW}} = 841.5$ MHz) signal fed into one of the transducers (IDT$_1$). The PL-intensity strongly decreases until at the highest power used it becomes completely quenched. This quenching is already an indirect indication of the increased trapping probability and subsequent transport of the e–h pairs, as will be demonstrated in the following.

In the moving potential superlattice with period $\lambda_{\mathrm{SAW}} = 3.4$ μm the excitons become polarized predominantly by the lateral electric field until they dissociate at high fields into spatially separated e–h pairs. These are then efficiently stored in the potential minima and maxima of the conduction and the valence band, respectively (see inset of Fig. 1). For an acoustic power of $P_1 = +13.5$ dBm (22.4 mW) lateral fields as high as $E_{\mathrm{l}} = 8$ kV/cm and vertical fields up to $E_{\mathrm{v}} = 10$ kV/cm are achieved [9]. The dramatically prolonged recombination time of the trapped e–h pairs together with the propagation of the SAW along the surface of the quantum well sample enable us to directly study the transport of the photogenerated carriers over macroscopic distances as sketched in the inset of Fig. 2. Deliberate screening of the storing lateral potential triggers radiative recombination and thus the reassembly of the polarized e–h pairs into photons. In this experiment, optical excitation and emission of the PL do not occur at

the same spot of the sample. Using a pulsed laser diode the optical excitation is accomplished at the site $x = x_{\text{in}}$, whereas the detector monitors the PL coming from a location $x = x_{\text{out}}$. The part of the sample beyond $x = x_{\text{out}}$ is covered by a thin, semitransparent nickel-chromium layer that readily screens the lateral piezoelectric fields of the SAW [11,13] and thus triggers recombination. At the time $t = 0$ a SAW pulse of width $\Delta t = 200$ ns is launched at the emitting IDT_1. At around $t = t_1$ the SAW pulse is centered at $x = x_{\text{in}}$ where a laser pulse creates excitonic excitations. These excitons are immediately field-ionized and the resulting electron–hole pairs are efficiently trapped in the moving lateral potential wells of the SAW as indirectly seen in Fig. 1. After an acoustic delay time of in this case $\tau_{\text{storage}} = 430$ ns corresponding to a transport path length of $x_{\text{out}} - x_{\text{in}} = 1.2$ mm the SAW pulse reaches the location $x = x_{\text{out}}$ where the lateral SAW fields are screened thus inducing recombination and a strong PL signal at the detector PM. Time delays τ_{storage} up to several μs corresponding to an e–h transport over some millimeters have been achieved without severe degradation of the transport efficiency, only the sample length imposing a maximum time delay.

The time-delayed PL is demonstrated in the lower part of Fig. 2. Here, we plot the PL intensity detected at $x = x_{\text{out}}$ as a function of time after the SAW excitation. The SAW and the pump laser pulses are indicated by the rectangles close to the ordinate. The decrease of the PL intensity at $t = t_1$ marks the arrival of the SAW pulse at the excitation site $x = x_{\text{in}}$ by quenching the direct and instantaneous PL at $x = x_{\text{in}}$ that is detected as weak stray light by the photomultiplier. To avoid any possible spurious effect originating from this stray light we make sure that the pump laser is switched off well before the SAW packet arrives at $x = x_{\text{out}}$. About 700 ns after the launch of the SAW pulse we detect a strong PL at the site $x = x_{\text{out}}$ which clearly indicates the SAW-mediated transport and subsequent recombination of the photogenerated carriers. Comparison of the PL that is detected at the pumping site x_{in} to the delayed PL at x_{out} shows that only about 30% of the photogenerated and trapped carriers are 'lost' along their way. The major mechanisms for this loss are believed to be non-radiative processes along the sound path which might be related to the high density of recombination centers at the mesa edges and to carrier tunneling through the barriers induced by the vertical piezoelectric fields.

We have shown that the electric fields associated with the piezoactive SAW can be strong enough to field-ionize photogenerated excitons and lead to a spatially separated storage of the resulting e–h 'fragments' in the moving potential superlattice. This ionization process of the excitons in the piezoelectric fields of the sound wave can be directly observed by the absorption of a second sound wave probing the areal conductivity of the photogenerated charges. SAW transmission experiments have been successfully used in the past as a sensitive probe of the dynamical sheet conductivity $\sigma(\omega, k)$ of a system of mobile carriers. So far, these experiments are focused on the conductivity of quasi two-dimensional electron systems (Q2DES) confined in semiconductor heterojunctions in the regime of the integer [11 to 13] and fractional [14] quantum Hall effect. Since the sensitivity of SAW transmission experiments is particularly high at very low sheet conductivities, they are well suited to study the conductivity related to the low-density optical excitations in an undoped quantum well.

The design of the sample is sketched in Fig. 3a. In addition to the interdigital transducers 1 and 2 with center frequencies $f_{1,2} = 841$ MHz used in the experiments described above, a second pair of IDTs with $f_{3,4} = 420$ MHz is defined on the sample. The four

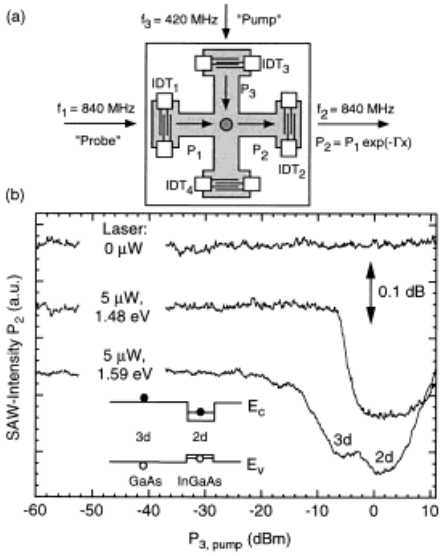

Fig. 3. a) Sample design for SAW-transmission experiments using four IDTs. b) Transmitted intensity of a 'probe' SAW as a function of the acoustic power P_1 of a 'pump' pulse. The variation of the sheet conductivity due to mobile carriers originating from ionization processes in the piezoelectric field of the 'pump' SAW results in an attenuation of the 'probe' SAW.

IDTs are placed at the ends of a cross-shaped mesa on the GaAs/InGaAs QW-structure used previously. A tunable titanium–sapphire laser is used for optical interband excitation of a $\pi(100\ \mu\mathrm{m})^2$-wide region at the center of the mesa. At $t = 0$ an acoustic 'pump' pulse ($\Delta t_{\mathrm{Pump}} = 400$ ns) is generated using IDT3 which then propagates in the direction of IDT4. In the middle of the mesa this 'pump' SAW intercepts a shorter 'probe' pulse from IDT1 ($\Delta t_{\mathrm{Probe}} = 200$ ns) that was generated at $t = 100$ ns. The acoustic power of the 'probing' SAW was kept below $P_1 = -40$ dBm throughout the experiment to exclude any dissociation processes of photogenerated excitons originating from the 'probe' pulse itself.

Fig. 3b depicts the transmitted SAW intensity P_2 of the 'probe'-pulse as a function of the acoustic power P_3 of the 'pump' SAW for different optical excitation energies and intensities. For clarity, we introduced an additional offset of 0.1 dB between the curves. For $I_{\mathrm{Las}} = 0$ no change of the intensity of the transmitted 'probe' pulse is observed as P_3 is increased. This reflects the expected unperturbed propagation and crossing of the two SAW pulses for a vanishing conductivity of the sample.

Optical excitation with energy $E_{\mathrm{Las}} = 1.48$ eV below the band gap of the GaAs barriers results in a selective population of the QW by photogenerated excitons. For low acoustic 'pump' powers P_3 the increase of the quasistatic sheet conductivity of the QW due to the polarization of these excitons is negligible. However, for $P_3 > -6$ dBm, corresponding to a lateral piezoelectric field strength of $E_{\mathrm{l}} \geq 600$ V/cm, the probability for the dissociation of the excitons by field-induced tunneling processes increases rapidly and is marked by a sharp onset of the absorption of the 'probe' SAW. This change in the SAW transmission can be understood in terms of the increased electrostatic screening of the 'probe' SAW potential by the mobile electrons and holes originating from the ionization process. The attenuation coefficient Γ of the 'probe' SAW is therefore related to the power dissipated by the local screening currents in the carrier system [11],

$$\Gamma = \frac{K_{\mathrm{eff}}^2}{2}\, k_{\mathrm{SAW}}\, \frac{\sigma/\sigma_{\mathrm{M}}}{1 + (\sigma/\sigma_{\mathrm{M}})^2}\,. \tag{1}$$

A further increase of the 'pump' power P_3 results in a smaller interaction between 'probe' SAW and mobile carrier system since its sheet conductivity now exceeds the critical conductivity $\sigma_{\mathrm{M}} \approx 3.4 \times 10^{-7}\ \Omega^{-1}$.

Optical excitation with $E_{\mathrm{Las}} = 1.59$ eV generates excitons both in the QW as well as in the GaAs barriers. The attenuation of 'probe' SAW intensity P_2 with increasing 'pump'- power P_1 now shows two distinct features and its onset is shifted to a smaller value $P_1 \approx -13$ dBm which corresponds to piezoelectric field strengths of 300 V/cm. This interaction at smaller 'pump'-powers P_1 can be attributed to the dissociation of the 3d- excitons in the GaAs barriers. Since the exciton binding energy of bulk GaAs ($\approx$4.2 meV) is considerably smaller than for the InGaAs-QW ($\approx$ 8 meV [15]) the piezoelectric field strengths and hence the acoustic power P_1 required to enable field induced tunneling processes will be smaller. Due to the variation of the SAW-induced piezoelectric field strength into the substrate, the dissociation rate of the 3d-excitons by field induced tunneling processes will also vary with depth. This results in the observed broadening of the onset of the 3d-excitonic feature in P_2 in comparison to the QW-exciton case. Acoustic powers P_1 above +4 dBm lead to a rapidly increasing density of mobile carriers and thus to an increasing conductivity $\sigma > \sigma_{\mathrm{M}}$ yielding a smaller attenuation Γ.

Acknowledgements. We gratefully acknowledge technical advise of S. Manus, and the financial support of the Deutsche Forschungsgemeinschaft (DFG) and the Bayerische Forschungsstiftung FOROPTO.

References

[1] S. Schmitt-Rink, D.S. Chemla, and D.A.B. Miller, Adv. in Phys. **38**, 89 (1989).
[2] D.A.B. Miller, D.S. Chemla, T.C. Damen, A.C. Gossard, W. Wiegmann, T.H. Wood, and C.A. Burrus, Phys. Rev. B **32**, 1043 (1985).
[3] See, e.g., IEEE J. Quantum Electron. **29**, 2 (1993); Spatial Light Modulators: Appl. Opt. **31**, 20 (1992); and Optical Computing: Appl. Opt. **31**, 26 (1992).
[4] See, e.g., C. Weisbuch and B. Vinter, Quantum Semiconductor Structures, Academic Press, San Diego 1991.
[5] G.H. Döhler, H. Künzel, D. Olego, K. Ploog, P. Ruden, and H.J. Stolz, Phys. Rev. Lett. **47**, 864 (1981).
G.H. Döhler, G. Hasnain, and J.N. Miller, Appl. Phys. Lett. **49**, 704 (1986).
[6] A. Schmeller, W. Hansen, J.P. Kotthaus, G. Tränkle, and G. Weimann, Appl. Phys. Lett. **64**, 330 (1994).
[7] S. Zimmermann, A.O. Govorov, W. Hansen, J.P. Kotthaus, C. Rocke, A. Wixforth, M. Bichler, and W. Wegscheider, Proc. of MSS-8, St. Barbara, 1997 to be published.
[8] C. Rocke, S. Zimmermann, A. Wixforth, J.P. Kotthaus, G. Böhm, and G. Weimann, Phys. Rev. Lett. **78**, 4099 (1997).
A. Wixforth, C. Rocke, S. Zimmermann, J.P. Kotthaus, G. Böhm, and G. Weimann, Proc. of MSS-8, St. Barbara, 1997 to be published.
[9] Y. Kim and W.D. Hunt, J. Appl. Phys. **68**, 4993 (1990).
[10] M.J. Hoskins and B.J. Hunsinger, Appl. Phys. Lett. **41**, 332 (1982).
W.J. Tanski, S.W. Merritt, R.N. Sacks, D.E. Cullen, E.J. Branciforte, R. D. Carroll, and T.C. Eschrich, *Appl. Phys. Lett.* **52**, 18 (1988).
[11] A. Wixforth, J. P. Kotthaus, and G. Weimann,Phys. Rev. Lett. **56**, 2104 (1986).
A. Wixforth, J. Scriba, M. Wassermeier, J.P. Kotthaus, G. Weimann, and W. Schlapp, Phys. Rev. B **40**, 7874 (1989).
[12] V.W. Rampton, K. McEnaney, A.G. Kozorezov, P.J.A. Carter, C.D.W. Wilkinson, M. Henini, and O.H. Hughes, Semicond. Sci. Technol. **7**, 641 (1992).
[13] C. Rocke, S. Manus, A. Wixforth, M. Sundaram, J.H. English, and A.C. Gossard, Appl. Phys. Lett. **65**, 2422 (1994).
[14] R. L. Willet, R. R. Ruel, K. W. West, and L. N. Pfeiffer, Phys. Rev. Lett. **71**, 3846 (1993).
[15] G. Duggan, K.J. Moore, K. Woodbridge, and Christine Roberts, Surface Sc. **228**, 310 (1990).